Sigma Journal of Engineering and Natural Sciences
Web page info: https://sigma.yildiz.edu.tr
DOI: 10.14744/sigma.2022.00098

Research Article

Design and development of a ball-screw and electrical motor driven industrial electromechanical cylinder

Mohammad Javad FOTUHI[1,*], Cenk KARAMAN[2], Zafer BİNGÜL[2]

[1]*Research and Development, KeramikMakina Sanayi veTicaret A.S, Türkiye*
[2]*Automation and Robotics Lab, Department of Mechatronics Engineering, Kocaeli University, Türkiye*

ARTICLE INFO

Article history
Received: 10 March 2021
Revised: 22 April 2021
Accepted: 13 May 2021

Keywords:
Electrical Ball-Screw Driven Industrial Cylinder Mechanism (BSDICM); Efficiency, Position Root Mean Square Error (PRMSE); Electromechanical Cylinder; Industrial Pneumatic Cylinder

ABSTRACT

This paper presents a study on the implementation of converting an industrial pneumatic cylinder into an electromechanical cylinder drivetrain using a ball-screw mechanism and stepper motor (ECDLSM). Due to the fact that pneumatic cylinders in the industry are generally used in on-off operating mode, electric actuators provide more precise motion control (position, speed, acceleration, and force) along with providing superior accuracy and repeatability. The mechanical and electrical efficiency, for ce, and pos ition err ors of the ECDLSM have been examined based on the position, velocity, and acceleration profiles to the cylinder mechanism with the established test setup which consists of a current and force sensor, incremental and linear encoders, and springs. The highest ratio of the force applied-double spring was performed to verify the accuracy of the analysis results by interpreting the force data and position errors collected from the ECDLSM. The analysis results show that the ECDLSM is very useful and flexible as much as its counterparts.

Cite this article as: Fotuhi M J, Karaman C, Bingül Z. Design and development of a ball-screw and electrical motor driven industrial electromechanical cylinder. Sigma J Eng Nat Sci 2022;40(4):822–830.

INTRODUCTION

An actuator is defined as a device that converts energy into motion and produces essentially rotational and linear motion [1]. Linear actuators are used in places where linear motion is required and are known for a wide range of applications in various industries including materials handling [2], military [3], agriculture, machine tools [4, 5], and industrial machinery. Linear actuators are generally divided into three main groups according to power sources, which can be selected as electric current, hydraulic fluid pressure, or pneumatic pressure.

The pneumatic and hydraulic linear actuator include a simple piston inside a hollow cylinder [6]. External air compressor or the pump moves the piston inside the cylinder housing, and with this increasing pressure, the cylinder

***Corresponding author.**
*E-mail address: mohammad.fotuhi@keramik.com.tr

This paper was recommended for publication in revised form by Regional Editor Osman Nuri Uçan

moves along the piston axis, which generates the required linear force [7]. It returns to its original initial length by providing a spring force or another fluid to the opposite side of the piston [8]. However, many components are needed to operate the pneumatic system, such as buffer tanks, valves, regulators, etc. Hydraulic linear actuators are very similar to pneumatic actuators, but a non-compressible fluid must be used as opposed to compressed air in which the cylinder is moved in a linear motion. Electric actuators consist of a ball, roller screw, or belt connected via a coupler to an electric motor. When the screw rotates, it moves the piston and the piston is connected to a rod or a carrier that moves the load. These actuators have some advantages and disadvantages according to the requirements of the process in which they will be used.

Medium and small-scale enterprises are switching to electrical actuators to expand their product portfolio by designing new products or converting existing pneumatic products. However, the switching to electric actuators is focused on achieving more precise and full-motion profile control (position, speed, acceleration/deceleration, and force) of electric actuators, as well as providing superior precision and repeatability and preventing vibration and noise in motion. While electric actuators are higher in performance and initial cost, studies have confirmed that the electric actuator solution makes it a more economical option than air cylinders over the life of the device or machine [9]. This reference shows that factors such as efficiency, electricity usage costs, air leakage, maintenance, product change, product quality, change time, and cycle times have been examined along with other factors that determine the total cost of ownership for a pneumatic actuator technology. Also, in terms of efficiency, it was found that only 23% - 30% for pneumatic systems, 40% for hydraulic systems, and 80% for electrical systems [10].

By comparison with others, electric actuators require little or no maintenance. Some actuators may require relubrication from time to time, but often electric actuators do not demand regular maintenance.

In electronic cylinder applications, the cylinder motion profile is designed by a user program. Therefore, the cylinder profile is very easy to change and significantly reduces time. This subject is discussed in many research articles [11, 12, 13]. In this paper, the application of the ECDLSM was developed from the switching of the existing pneumatic cylinder. The main goal of such a system is to avoid the force overshoots in the contact stage while keeping stress force error in the high-sensitive tracking stage, where traditional pneumatic cylinders are not competent. The content flow of this paper is organized as follows: First, the modeling of electromechanical CDLSM is briefly introduced, and the mechanical design is presented, next, the simulation and experimental results are given and discussed in detail. Finally, the conclusions are summarized.

MODELING OF ELECTROMECHANICAL CDLSM

The switched electric actuator consists of three units: motor unit, coupling unit, driver unit. A hybrid stepper motor with two-phase was used in the experimental study because it is advantageous in applications where rotation angle, speed, position, and synchronism need to be controlled. Stepper motors are used in many different applications [6, 7]. For the coupling unit, acme ball screw and nut system were preferred as the price is affordable and easy to find in small dimensions. The screw was integrated into the rotor of the stepper motor to prevent vibration during the acceleration and deceleration phases of the motion. The linear encoder attached to the moving piston and the rotary encoder attached to the stepper motor were used to validate the test system and to implement the control algorithm. A visual C ++ based program has been developed to enter motion profile and control signals using an industrial PC (Googoltech) with many analog/digital input/output ports. In order to analyse the linear force generated by the system, springs with three different stiffness coefficients were used. Using different speed and motion profiles, the force values produced by the system, the current value drawn by the motor, the maximum acceleration, speed and force values achieved at these speeds were determined.

The diagram of the ECDLSM is illustrated in Figure.1. For the ECDLSM, a model was developed in [14, 15]. The

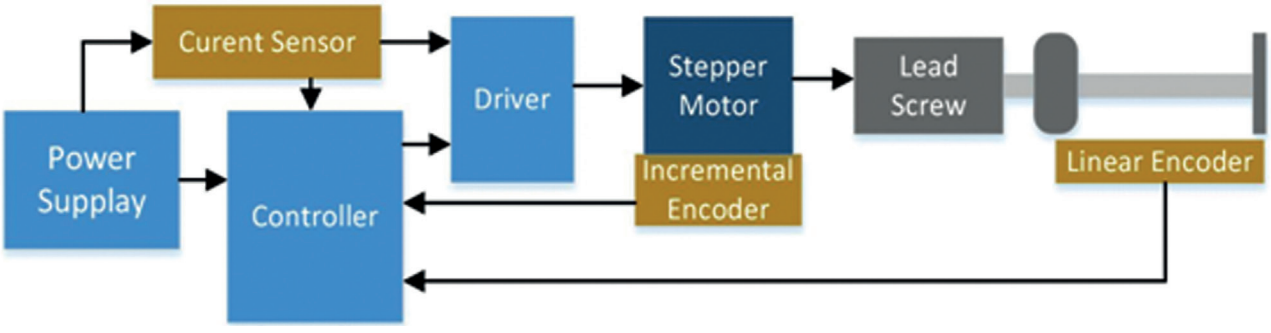

Figure 1. Block diagram of the ECDLSM.

mathematical model is based on two movements, the motor angle θ and the distance of load. The θ angle is linked by a ball screw mechanism to the d distance.

According to the change of position, two forces are formed at the input and output of the system. a motor forces Fm applied at the input of the system and a load forces Fl applied at the output of the system.

MECHANICAL DESIGN

To obtain a simple and cheap design, we minimized the amount of mechanical and electronic parts. It was therefore decided to use normal stepper motor and ball-screw. Also, electromechanical cylinder can be both opened and closed by only one HANPOSE 17HS3401S T8 × 8 nema-stepper motor with a PK65N ball-screw driven by the stepper motor driver model CWD556. When a voltage of 24V is applied to the motor this results in a constant actuation torque of 0.5 Nm applied at the base of end effector and 0.25Nm on each of the opposite link as defined [16].

The torque general equation (1) was used to obtain the ball-screw dynamic equations. General force F was calculated by sum of two different forces; the torque caused by frictional forces *fr* and the torque of external forces applied to the shaft.

$$T = \frac{FL}{2\pi v} \tag{1}$$

$$\beta = \frac{L}{D_p - \left(\frac{P_B}{2}\right)} \tag{2}$$

$$F = F_A + mg(sin\theta + \mu cos\theta) = F_A + fr \tag{3}$$

$$T_{BS} = \frac{(F_A + fr)\, P_B}{2\pi i}\left(\frac{1}{\eta} + \frac{1}{3}\mu_0\right) \tag{4}$$

Here, F is the Force along the direction of movement (see Figure .2), F_A is the external force, θ is the tilt-angle (degree), D_p is the pitch circle diameter (9.5 mm), D_r is the root diameter of the screw shaft, P_B is the screw pitch (5 mm), L is the lead of the thread (5 mm), n_s is the number of starts (1), μ is the friction coefficient of sliding surface, μ_0 is the internal friction coefficient of preload nut (0.15),

Figure 2. Model of the ball-screw.

η is the efficiency, α is the thread angle for a standard bolt (30 degree) [17, 18]. The torque general equation (4) was used to obtain the ball-screw dynamic equations. The T_{BS} is general torque term on the ball-screw use in equation (5).

RESULTS AND DISCUSSION

There are several methods for analyzing and measuring force, three spring with different stiffness coefficient values (Table 1) has been used to analyze the dynamic behavior of the system [19]. To analyze the ECDLSM, two sensors used to measure data, sensors are incremental encoder of motor and load-linear encoder [20,21], motor incremental encoder gives a pulse output of 0.17578125 (degrees/pulse), and load linear encoder gives a voltage output of 0.5 (mV/mm), over the range0-20 mm this is amplified by an amplifier with voltage gain of 20, sampled and applied to a 10-bit analog-to-digital converter with voltage range 0-5 V. resolution of the measurement is 1024 (Digital value/mm). The experimental setup of electrical ECDLSM is shown in Figure.3. The position and current analog signals are converted to physical parameters by using sensor gains (equation 6, 7, 8), they are given in Table 1.

$$D_L(\text{mm}) = (V_L - o_v) * (c_V) \tag{5}$$

$$D_M(\text{mm}) = (P_M - o_p) * (c_P^{-1}) \tag{6}$$

$$C_s(\text{Amper}) = (V_c - o_c) * (c_c^{-1}) \tag{7}$$

Here D_L is the distance of load (mm), D_M is the distance of linear movement of motor (mm), C_s is the equation of current sensing, V_L is the digitized voltage from analog to digital using an ADC (analog to digital converter) value of voltage output of the load linear encoder (digital value), P_M is the pulse number of the motor incremental encoder (pulse), V_C is the discrete voltage (ADC value of voltage) output of the current sensor.

Table 1: position and current sensors gains

Parameter	Symbol	Value	Unit
voltage coefficient of the linear encoder	c_V	1.3852	mm/volt
pulse coefficient of the incremental encoder	c_P	1.0104	mm/pulse
current coefficient of the current sensor	c_C	28.8921	amper/volt
offset of voltage	o_V	781.3157	volt
offset of pulse	o_P	61.2864	pulse
offset of current	o_C	16.8264	amper

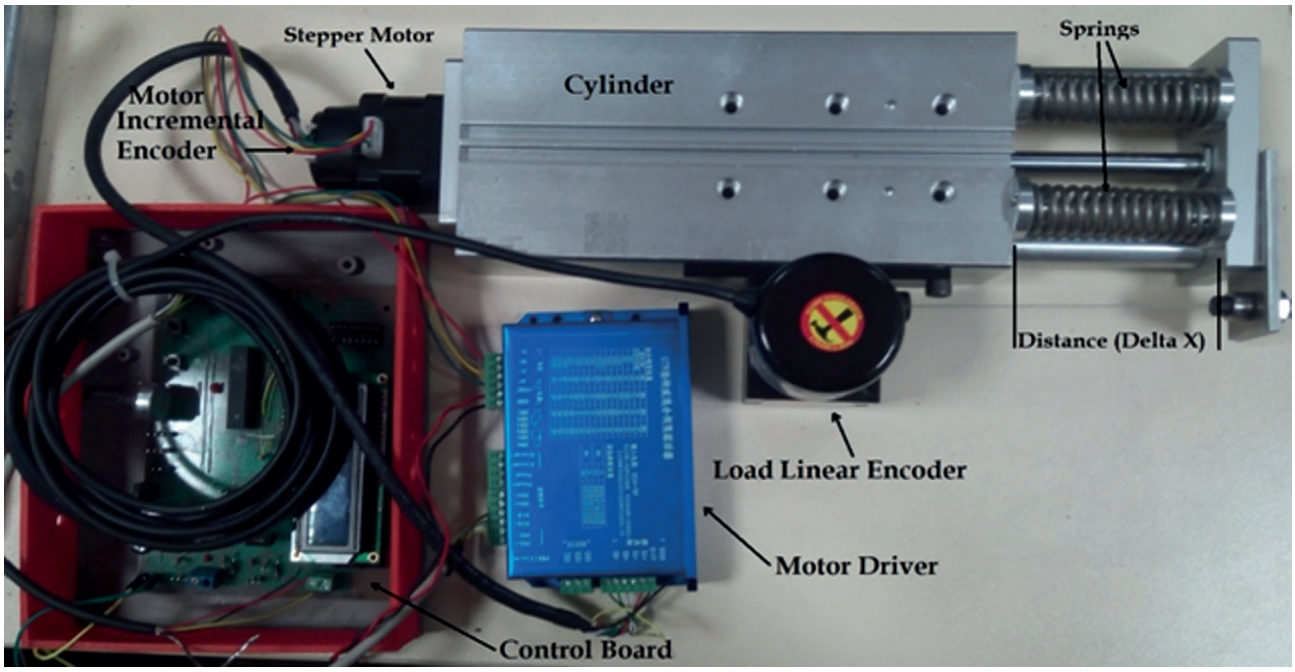

Figure 3. Experimental setup of ECDLSM.

Table 2-Technical specification of springs

Spring type	Stiffness (Ks= N/mm)	Free length (mm)	Full compression (mm)	Total coil
A	4.529	67.47	21.33	10
B	4.813	70.68	36.63	15
C	6.016	67.43	30.17	12

Table 3-Velocity profile (Max of speed = 42 mm/s)

Speed Mode	Speed	Speed (mm/s)
Low Speed	9 % Max	3.78
Medium Speed	55 % Max	23.10
High Speed	80 % Max	33.60
Very High Speed	90 % Max	37.80

To avoid repetition of showing same behavior in the paper, the movement profile of a Cylinder A-type of the spring in the low-speed case is only illustrated in the Figure 4. The results of the medium, high and very high speed of double-B and C types Springs of the springs for the ECDLSM are given also in Table 2. The velocity profile is shown in Table 3.

According to Table 4, For the A-type spring, the maximal force of 106.4 N and the maximum linear movement of 18.55 mm are obtained by the high velocity of 5.892 mm/sec. For the B-type spring, the maximal force of 100 N and the maximum linear movement of 9 mm are obtained by the high velocity of 1.375 mm/sec. For the C-type spring, the maximal force of 105 N and the maximum linear movement of 8,013 mm are obtained by the high velocity of 1.375 mm/sec.

In order to evaluate the performance of position errors, in general, the square root of the mean of all square errors (PRMSE) is calculated between the stepper motor position and the measured load signal based on Equation 9 [22, 23]. According to Table 5, the equations (10, 11) are used to illustrate the effect of time and magnitude of the error in Equation 9.

$$\mathrm{PRMSE} = \sqrt{\frac{1}{N}\sum_{i=1}^{N}(p_i - \hat{p}_i)^2} \tag{9}$$

Integral of the square value of the error (ISE):

$$\mathrm{ISE} = \sum_{i=1}^{N}(p_i - \hat{p}_i)^2 \tag{10}$$

Sigma J Eng Nat Sci, Vol. 40, No. 4, pp. 822–830, December, 2022

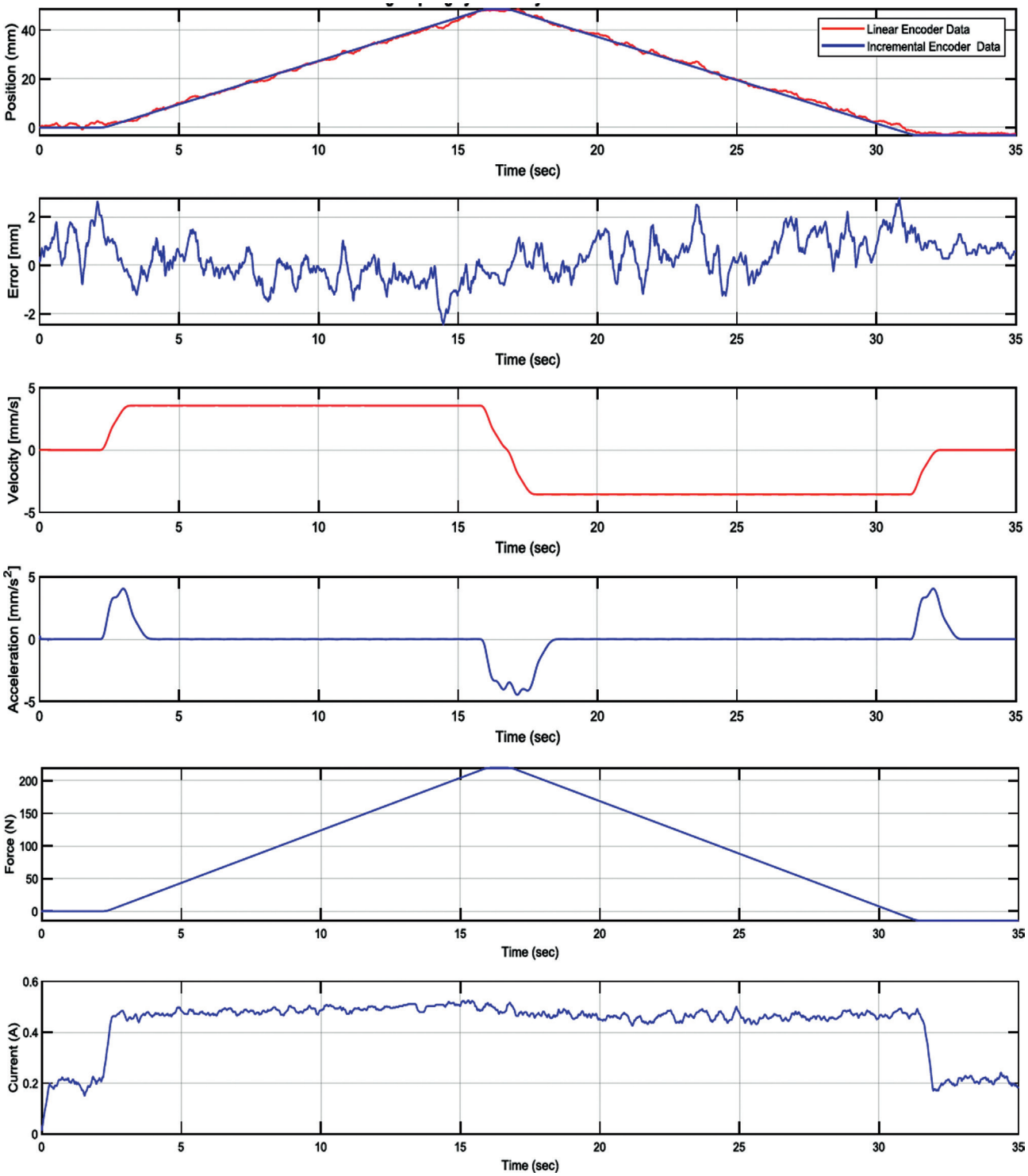

Figure 4. The motion profile of double A- type Spring in the low-speed case.

Table 4. ECDLSM and double spring motion analysis

Spring type	Speed mode	Max linear movement (mm)	Max Force (N)	Time (sec)	Max Current (A)	Max Velocity (mm/sec)	Max Acceleration (mm/sec^2)
A	Low	39.67	359.4	25.94	0.4657	3.56	4.035
	Medium	33.88	307.8	4.11	0.9664	21.26	23.93
	High	26.48	241.8	2.535	0.9155	30.19	36.2
	Very High	15.07	137.8	2.175	0.6914	21.53	37.14
B	Low	34.08	324.9	24.02	0.5505	3.559	3.744
	Medium	30	288.8	3.825	0.9647	20.83	22.77
	High	23.14	223	3.465	0.9053	28.52	49.84
	Very High	12.96	127.7	2.58	0.6031	36.53	137.3
C	Low	27.22	327.5	22.065	0.52	3.557	10.89
	Medium	23.82	290.2	3.75	0.9647	21.25	70.99
	High	18.7	224.5	3	0.8866	27.22	111.5
	Very High	10.6	127.5	5.25	0.6439	15.9	82.24

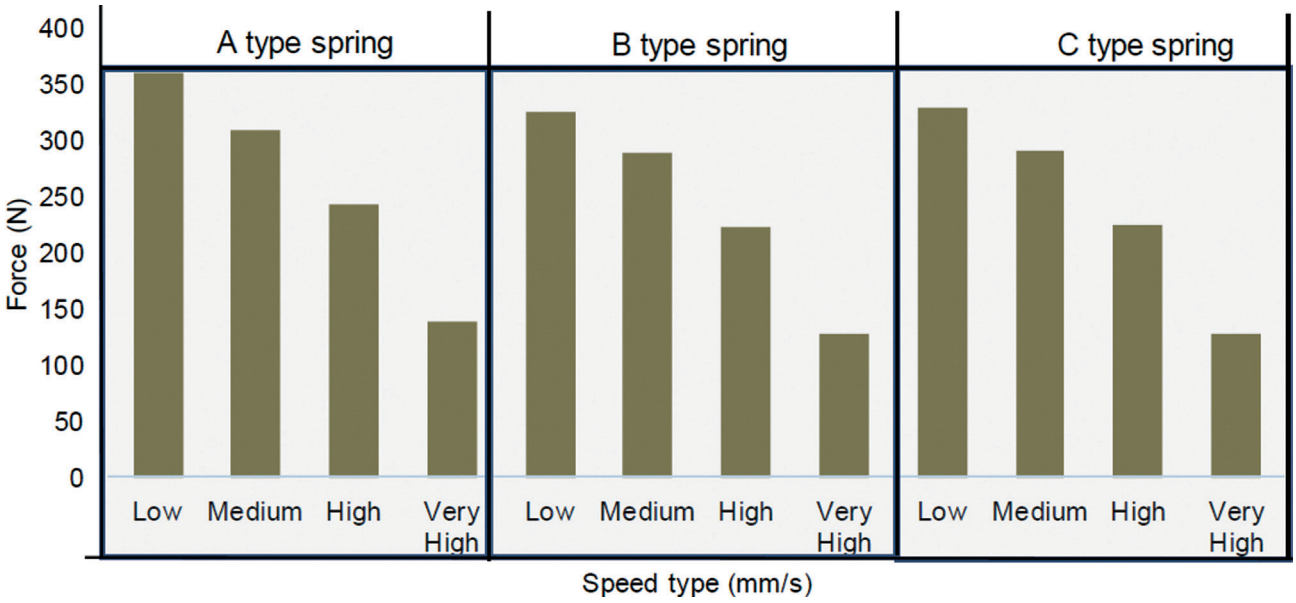

Figure 5. Force analysis results for A, B and C types double springs.

Table 5. RMS position error (ISE and ITSE method) comparison of different speed cases (unit: mm) note: (A, B and C types double-spring)

Speed mode	Double spring (ISE)			Double spring (ITSE)		
	A	B	C	A	B	C
Low	0.0722	0.0146	0.0092	1.4417	0.2779	0.1118
Medium	0.0991	0.0191	0.0117	0.2974	0.0384	0.0233
High	0.1060	0.0192	0.0210	0.2040	0.0319	0.0417
Very high	0.1065	0.0215	0.0358	0.2134	0.0264	0.0979

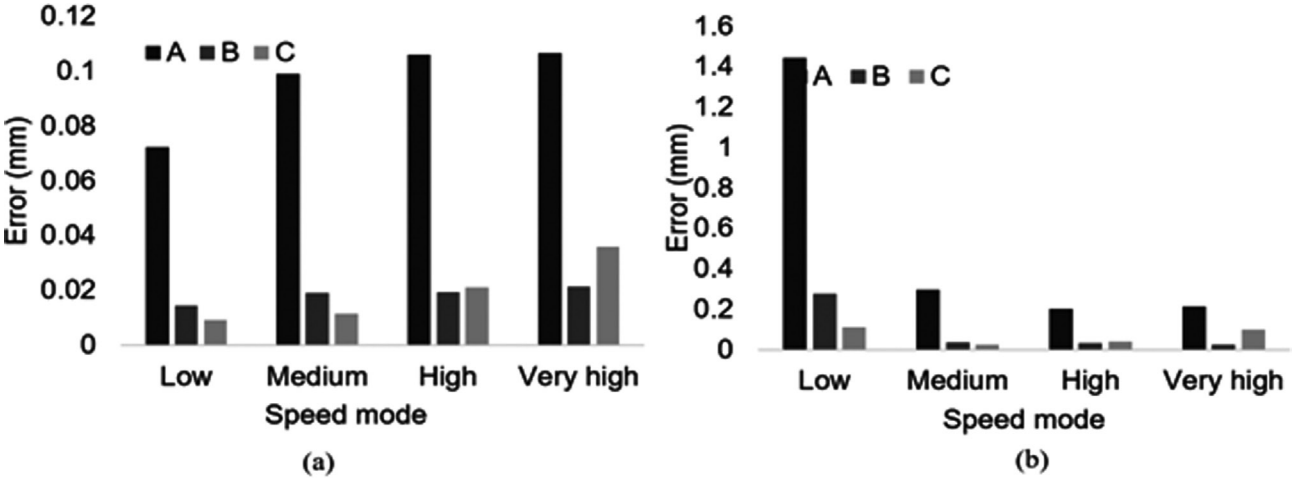

Figure 6. The PRMSEs of different speed cases with (A, B and C)-types double spring, (a) ISE (b) ITSE.

Integral of the time weighted square value of the error (ITSE):

$$\mathrm{ITSE} = \sum_{i=1}^{N} t(\mathrm{p_i} - \hat{\mathrm{p}}_i)^2 \tag{11}$$

Where $\mathrm{p_i}$ is the output position, $\hat{\mathrm{p}}_i$ is the input position, t is the sampling time and N is the sampling number [24, 25].

To evaluate the performance of the maximum force of the electrical CDLSM, the ratio of the maximum force (RMF) between the desirable force (F_d) and the measured force (F_m) of the system is calculated based on the following equation (12) [27], As can be seen Table 4, the RMF is the highest ratio of the force applied by the system to the spring.

$$\mathrm{RMF} = \left(1 - \left(\frac{F_d - F_m}{F_d}\right)\right) * 100 \tag{12}$$

The highest ratio of the force applied by the system to the A-type spring is 89.51% obtained by the low velocities of 3.78 mm/s. It can be seen that in Table 6 the lowest values are related to the fourth row of speeds (very high) which are less than 50% and the values are unacceptable, indicating that the system did not respond correctly at this speed. According to Table 4, and applying speeds from Table 6, the highest power for cylinder is 1.96 watt (A- HS) [28].

For three springs with different stiffness coefficient values, the force analysis of cylinder is given in Table 4. According to the diagrams of Figures 5 and 6, compared to the magnitude of the error of the cylinders and the force produced by them, the output force of the cylinder is constant on average (337 N) at the velocities of 3.78 mm/s. The best cylinder efficiency with a A-type spring stiffness of 4.529 at a velocity of 3.78 mm/s, which is 89.51%.

CONCLUSION

In this paper, an experimental setup for the ECDLSM was designed and developed. In the experimental setup, the force was calculated based on the spring's stiffness. The forces of the ECDLSM were analyzed using the position errors obtained from the load and stepper motor position. In order to evaluate the ECDLSM for different forces, three springs with different stiffness coefficient values were used for the force analysis. The RMSE between the position of the stepper motor and the position measured signal of the load was calculated for the position performance of the system. In the high-velocity case with A-type spring, the minimum RMSEs values were obtained as expected. The max force value (F=359 N) was obtained by the ball-screw mechanism and stepper motor. The results show that the A-type spring-cylinder performed better than the B and C-type spring-cylinder and the highest ratio of the force applied by the proposed RMF method is 89.51% at 3.78 mm/s. This prototype of the ECDLSM developed here can be enhanced using the stepper motor with high power and high position accuracy. In this way, the position errors that occurred here may be eliminated very easily.

DECLARATION OF COMPETING INTEREST

The authors declare that they have no known competing financial interests or personal relationships that could have appeared to influence the work reported in this paper.

AUTHORSHIP CONTRIBUTIONS

Authors equally contributed to this work.

DATA AVAILABILITY STATEMENT

The authors confirm that the data that supports the findings of this study are available within the article. Raw

data that support the finding of this study are available from the corresponding author, upon reasonable request.

CONFLICT OF INTEREST

The author declared no potential conflicts of interest with respect to the research, authorship, and/or publication of this article.

ETHICS

There are no ethical issues with the publication of this manuscript.

REFERENCES

[1] Zhou HX, Zhou CG, Feng HT, Ou Y. Theoretical and experimental analysis of the preload degradation of double-nut ball screws. Precis Eng 2020;65:72–90. [CrossRef]

[2] Hagen D, Pawlus W, Ebbesen MK, Andersen TO. Feasibility study of electromechanical cylinder drivetrain for offshore mechatronic systems. Model Identif Control 2017;38:59–77. [CrossRef]

[3] Rouhi M, Ghayoor H, Fortin-Simpson J, Zacchia TT, Hoa SV, Hojjati M. Design, manufacturing, and testing of a variable stiffness composite cylinder. Compos Struct 2018;184:146–152. [CrossRef]

[4] Liu Y, Gao X, Yang X. Research of control strategy in the large electric cylinder position servo system. Math Probl Eng 2015:1–6. [CrossRef]

[5] Li X, Chen W, Lin W, Low KH. A variable stiffness robotic gripper based on structure-controlled principle. IEEE Trans Autom Sci Eng 2017;15:1104–1113. [CrossRef]

[6] Thöndel E. Linear electromechanical actuator as a replacement of hydraulic cylinder for electric motion platform for use in simulators. In: Mastorakis NE, editor. Recent researches in applied informatics : Proceedings of the 2nd International conference on Applied Informatics and Computing Theory (AICT'11); 2011 Sept 26-28; Prague, Czech Republic: WSEAS; 2011. pp. 290–295.

[7] Kumar R, Mehta U, Chand P. A low cost linear force feedback control system for a two-fingered parallel configuration gripper. Procedia Comput Sci 2017;105:264–269. [CrossRef]

[8] Martin GE. On the theory of segmented electromechanical systems. J Acoust Soc Am 1964;36:1366–1370. [CrossRef]

[9] Datta R, Pradhan S, Bhattacharya B. Analysis and design optimization of a robotic gripper using multiobjective genetic algorithm. IEEE Trans Syst Man Cybern Syst 2015;46:16–26. [CrossRef]

[10] Najjari B, Barakati SM, Mohammadi A, Futohi MJ, Bostanian M. Position control of an electro-pneumatic system based on PWM technique and FLC. ISA Trans 2014;53:647–657. [CrossRef]

[11] Turner AJ, Ramsay K. Review and development of electromechanical actuators for improved transmission control and efficiency. SAE Trans 2004;1:908–919. [CrossRef]

[12] Rigacci M, Sato R, Shirase K. Experimental evaluation of mechanical and electrical power consumption of feed drive systems driven by a ball-screw. Precis Eng 2020;64:280–287. [CrossRef]

[13] Zhang LC, Zu L. A new method to calculate the friction coefficient of ball screws based on the thermal equilibrium. Adv Mech Eng 2019;11:1–5. [CrossRef]

[14] Park TM, Won SY, Lee SR, Sziebig G. Force feedback based gripper control on a robotic arm. 2016 IEEE 20th Jubilee International Conference on Intelligent Engineering Systems (INES); 2016 June 30-Jul 2; Budapest, Hungary: IEEE; 2016. pp. 107–112. [CrossRef]

[15] Liu Y, Zhang Y, Xu Q. Design and control of a novel compliant constant-force gripper based on buckled fixed-guided beams. IEEE/ASME Trans Mechatron 2017;22:476–486. [CrossRef]

[16] Xu F, Wang B, Shen J, Hu J, Jiang G. Design and realization of the claw gripper system of a climbing robot. J Intell Robot Syst 2018;89:301–317. [CrossRef]

[17] Rateni G, Cianchetti M, Ciuti G, Menciassi A, Laschi C. Design and development of a soft robotic gripper for manipulation in minimally invasive surgery: a proof of concept. Meccanica 2015;50:2855–2863. [CrossRef]

[18] Hagen D, Padovani D, Choux M. Guidelines to select between self-contained electro-hydraulic and electromechanical cylinders. 2020 15th IEEE Conference on Industrial Electronics and Applications (ICIEA); 2020 Nov 09-13; Kristiansand,Norway: IEEE; 2016. pp.547–554. [CrossRef]

[19] Fotuhi MJ, Yılmaz O, Bingul Z. Human postural ankle torque control model during standing posture with a series elastic muscle-tendon actuator. SN Appl Sci 2020;2:1–8. [CrossRef]

[20] Fotuhi MJ, Hazem ZB, Bingül Z. Modelling and torque control of an non-linear friction inverted pendulum driven with a rotary series elastic actuator. In: Ozseven T, Yasar E, editors. 3rd International Symposium on Multidisciplinary Studies and Innovative Technologies (ISMSIT); 2019 Oct 11-13; Ankara,Turkiye: IEEE; 2019. [CrossRef]

[21] Frey S, Dadalau A, Verl A. Expedient modeling of ball screw feed drives. Prod Eng 2012;6:205–211. [CrossRef]

[22] Li Q, Qin Q, Zhang S, Deng H. (2011) Optimal design for heavy forging robot grippers. Appl Mech Mater 2011;44-47:743–747. [CrossRef]

[23] Vicente DA, Hecker RL, Villegas FJ, Flores GM. Modeling and vibration mode analysis of a ball screw drive. Int J Adv Manuf Technol 2012;58:257–265. [CrossRef]

[24] Wilkinson LJ, Summer MD, Rust JB, Bosscher PM. High-force robotic gripper. U.S. Patent 8,534,729. Florida: Harris Corporation; 2013.

[25] Chen CL, Jang MJ, Lin KC. Modeling and high-precision control of a ball-screw-driven stage. Precis Eng 2004;28:483–495.

[26] Varanasi KK, Nayfeh SA. The dynamics of lead-screw drives: low-order modeling and experiments. J Dyn Sys Meas Control 2004;126:388–396. [CrossRef]

[27] Heilala J, Ropponen T, Airila M. Mechatronic design for industrial grippers. Mechatronics 1992;2:239–255. [CrossRef]

[28] Sato R. Sensor-less estimation of positioning reversal value for ball screw feed drives. Precis Eng 2019;60:116–120. [CrossRef]